

# Design and enhancement of microstrip patch antenna with frequency selective surface backing for vehicle-to-vehicle communication

**Ikram Troudi<sup>1</sup>, Chokri Baccouch<sup>2</sup>, Rhaimi Belgacem Chibani<sup>1</sup>**

<sup>1</sup>MACS Laboratory: Modeling, Analysis and Control of Systems LR16ES22, National Engineering School of Gabes, University of Gabes Gabes, Tunisia

<sup>2</sup>LR-Sys'Com-ENIT, Communications Systems LR-99-ES21, National Engineering School of Tunis, University of Tunis, Tunis, Tunisia

## Article Info

### Article history:

Received Mar 27, 2024

Revised Jul 25, 2024

Accepted Aug 6, 2024

### Keywords:

Bandwidth

Frequency selective surface

Gain enhancement

Patch antenna

Vehicle-to-vehicle

communications

## ABSTRACT

This research investigates the application of frequency selective surface (FSS) reflectors to enhance vehicle-to-vehicle (V2V) communication performance. A compact antenna measuring 32×24×1.6 mm, derived from an FSS 10×10×1.6 mm unit cell, was studied. Integration of FSS technology with the antenna resulted in significant performance improvements. The gain increased from 3.9 to 5.4 dB at 5.9 GHz, representing a 1.5-fold enhancement. Additionally, the bandwidth extended to 230.94 MHz. These advancements demonstrate the efficacy of FSS technology for antenna gain enhancement in V2V systems. The compact design, coupled with improved performance, makes this approach particularly suitable for vehicular applications where space is limited. This study not only showcases the potential of FSS technology in antenna design but also suggests its broader applicability in enhancing V2V communication systems, potentially contributing to the development of more efficient and safer transportation networks.

This is an open access article under the [CC BY-SA](https://creativecommons.org/licenses/by-sa/4.0/) license.



## Corresponding Author:

Chokri Baccouch

SYS'COM Laboratory LR99ES21, National Engineering School of Tunis, Tunis El Manar University

1002, Tunis, Tunisia

Email: chokri.baccouch13@gmail.com

## 1. INTRODUCTION

Throughout history, numerous studies have been conducted to discover efficient antennas capable of meeting the increasing demand for advanced communication. These antennas must possess characteristics such as large bandwidth, high gain, directional radiation, ease of manufacturing, and affordability [1], [2]. In order to increase antenna gain, a number of techniques have been widely used. Epsilon-near-zero (ENZ) materials are one such technique [3]–[5]. Altering the patch geometry [6], [7] or adding a superstrate, like an electromagnetic band gap (EBG) [8], [9], are two further strategies. Furthermore, we suggest the method of putting a frequency selective surface (FSS) reflector behind the antenna in order to increase the gain even more [10]–[12]. Electromagnetic waves are effectively reflected in phase by this reflector [13]. The FSS cell is used to create antenna reflectors and spatial filters in radar systems, communication systems, antenna technology, and mobile communication [14]. Planar and infinite, FSS structures can reflect plane waves in phase because of their high impedance [15].

In [16], a novel design for a printed antenna patch is proposed, specifically tailored for 5G applications. A FSS positioned  $\lambda/4$  behind the antenna, acting as a reflector, is part of the suggested design. At 3.5 GHz, this configuration greatly increases the antenna's gain by 9.12 dB.

Moving on to [17], a new filter structure is shown. It consists of a planar layer with a 3×3 cell array of FSS transmitters. At a frequency of 3.5 GHz, this filter is smoothly integrated with an ultra-wideband (UWB) antenna, preserving a separation distance of 10 mm. This integration's main goal is to successfully shield signals in UWB wireless applications, especially for connected items using 5G technology.

Daghari and Sakli [18] proposed a cylindrical filter antenna designed specifically for vehicular communication at a frequency of 5.9 GHz. The antenna's performance was enhanced by an array of FSS reflectors inside the cylindrical structure, resulting in a 1.5 dB gain increase. In contrast, a novel UWB antenna design was investigated in [19], incorporating a dual-polarized radiator and a back reflector with a single FSS. This integration of FSS enabled the antenna to achieve an impressive gain of 9.5 dB. In the publication [20], the utilization of a circular ring with three straight legs has been demonstrated to enhance the impedance bandwidth of the antenna. This improvement allows for a broader range of frequencies, spanning from 2.1 to 12.6 GHz, while also achieving superior return loss performance. The incorporation of three straight legs into the circular ring structure, forming a pattern resembling the Mercedes logo, functions as an impedance matching circuit. By carefully adjusting the spacing between the coplanar waveguide (CPW) and the feed line, the input impedance can be finely tuned, resulting in a 10 dB return loss bandwidth. This particular configuration ensures a more consistent gain across the ultra-wideband (UWB) frequencies and facilitates a high radiation efficiency of approximately 97% within the operational frequency range.

In the research conducted in [21], a comprehensive investigation is presented on a millimeter-wave (mm-wave) antenna specifically designed for 5G networks. The antenna incorporates a rectangular slot and is further enhanced with a FSS to enhance its gain. The proposed millimeter-wave antenna for 5G networks has successfully achieved a bandwidth with  $S_{11} \leq -10$  dB ranging from 25.5 to 30.8 GHz, along with a realized gain of approximately 10.3 dBi at 28 GHz. On the other hand, the antenna lacking FSS-based reflectors has attained a bandwidth with  $S_{11} \leq -10$  dB spanning from 26 to 29.8 GHz, accompanied by a realized gain of roughly 4.5 dBi across the entire frequency spectrum.

The application of FSS patch antennas in vehicle-to-vehicle (V2V) communication signifies a notable progression owing to their distinctive attributes tailored to meet the specific demands of this evolving technology [22]. FSS patch antennas offer a multitude of advantages, encompassing amplified gain for stronger and more reliable vehicle connections, enhanced directivity that precisely concentrates signals where required, and diminished multipath propagation to minimize signal distortion and augment overall system performance [23], [24]. Their compact dimensions enable seamless integration into vehicles without compromising functionality, while their streamlined design contributes to improved aerodynamics and fuel efficiency. Furthermore, the cost-effectiveness of FSS patch antennas, achieved through uncomplicated manufacturing processes and affordable components, renders them a practical choice for large-scale production. Collectively, these features position FSS patch antennas as an optimal solution for facilitating dependable and efficient wireless communication among vehicles in V2V systems, thereby paving the way for enhanced road safety and driving experiences [24].

Our paper introduces a novel approach where an array of FSS is integrated with a proposed antenna. The FSS unit cell design resembles a crescent moon shape, with dimensions of 10×10 mm, corresponding to  $\lambda/5 \times \lambda/5$ , where  $\lambda$  represents the wavelength. Furthermore, the suggested FSS displays a stop band characteristic within the 5.9 GHz range, resulting in a significant gain enhancement of up to 4.2 dB. Positioned  $\lambda/2$  below the antenna, the FSS contributes to the heightened gain. This enhancement occurs by reflecting and combining the antenna-emitted wave with the FSS-emitted wave. Maximum gain is achieved through constructive interference when these two waves are in phase. Empirical findings provide support for this conclusion.

The remaining sections of the document are organized as follows: section 2 presents the design and simulations of the antenna element. Section 3 discusses the geometry of the proposed FSS unit cell. In section 4, an 8×8 periodic arrangement of the FSS is utilized as a reflector to enhance gain, and the simulation results of the antenna with and without the FSS are compared. Section 5 is dedicated to the validation of the circuit electrically with advanced design system (ADS). This is a crucial step to ensure the functionality and reliability of the design. Finally, section 6 provides the concluding remarks of the paper, summarizing the key findings and potential future directions.

## 2. THE PROPOSED DESIGN

### 2.1. Design of proposed patch antenna

Figure 1 illustrates the geometry of a simple patch antenna with the following dimensions [25], [26]: length  $L=24$  mm, width  $W=32$  mm, and substrate thickness  $h=1.6$  mm. The antenna is constructed on an FR4 substrate, which has a relative permittivity of 4.3 and a loss tangent of 0.025.

$$L_p = \frac{c}{2f_r} \sqrt{\frac{2}{\epsilon_r + 1}} \quad 12.26 \text{ mm} \tag{1}$$

$$W_p = \frac{c}{2f_r \sqrt{\epsilon_r}} \quad 15.61 \text{ mm} \tag{2}$$

The dimensions of patch antenna proposed are given in Table 1 and Figure 2 shows the reflection parameter S11 of the patch antenna proposed as a function of frequency.

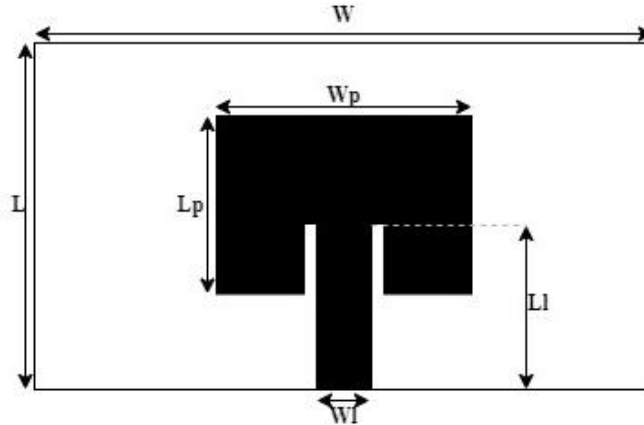


Figure 1. Patch antenna proposed

Table 1. Parameters of patch antenna

Parameters	L	W	L <sub>p</sub>	W <sub>p</sub>	L <sub>l</sub>	W <sub>l</sub>	h	T
Value (mm)	24	32	11.66	15.61	5	10	1.6	0.035

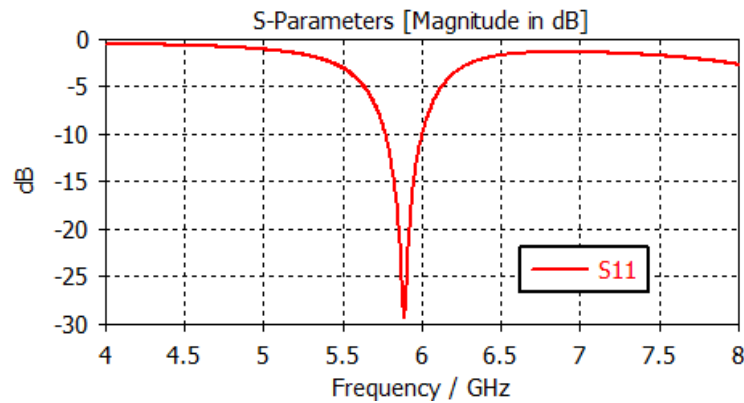


Figure 2. Reflection coefficient of proposed antenna

**2.2. Design of proposed frequency selective surface**

Figure 3 illustrates the dimensions and structure of the FSS crescent moon unit cell. This novel design functions as a reflector, redirecting electromagnetic waves towards a primary operating lobe. The proposed FSS is fabricated utilizing a Rogger RT5880 substrate, characterized by a loss tangent of 0.02, a dielectric constant of 2.2, and a thickness of 1.6 mm. The unit cell consists of two circular rings, with ring 1 having a radius of 9.75 mm and ring 2 having a radius of 8.5 mm. Increasing the radius results in a decrease in both the resonant frequency and the bandwidth. The FSS itself has dimensions of 10×10 mm (L×L). The reflection parameter S11 and the transmission coefficient of the FSS reflector can be observed in Figure 4. The FSS comprises an 8×8 array of cells, each measuring 80×80 mm, with a periodicity of 10 mm. The dimensions of the cells other than the periodicity match those of the entire array.

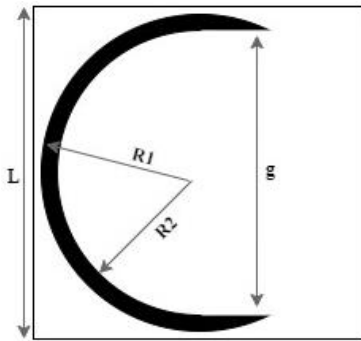


Figure 3. Design FSS proposed

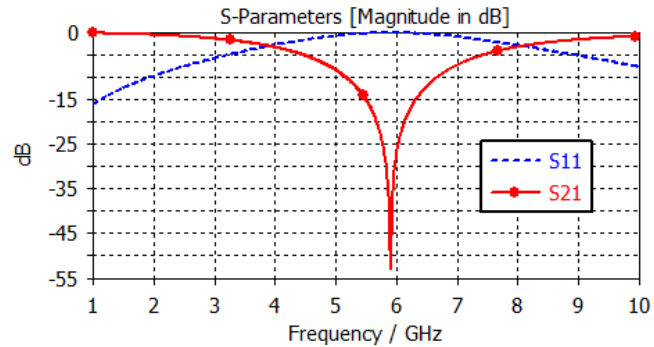


Figure 4. Reflection S11 and transmission S21 coefficient of FSS

### 3. RESULT AND DISCUSSION

This section presents a thorough examination of the reflection coefficients, radiation pattern, and gain of the patch antenna. The placement of an FSS array behind the antenna is shown in Figure 5. For optimal reflection, the distance between the proposed antenna and the FSS array should be  $\lambda/2$ , where  $\lambda$  is the wavelength corresponding to the resonant frequency of 5.9 GHz at the center.

The patch antenna emits a wave that radiates both upwards from the patch and downwards through the partial ground plane. A reflector made of FSS cells is placed at a distance of  $\lambda/2$  from the antenna, which redirects the downward wave back to the antenna, acting as an additional source of emission. Therefore, two waves are combined within the antenna: the primary wave from the patch and the secondary wave from the reflector, which travels a distance of  $\lambda$  after reflection. These waves are in phase and interfere constructively. As a result, the radiation pattern shifts, becoming omnidirectional above the patch. This enhancement contributes to improve both the antenna's directivity and gain. Furthermore, when the antenna is integrated into an electronic circuit, it also functions as an electromagnetic shield for the ground plane.

Figure 6 illustrates the reflection coefficient (S11) of the proposed antenna, both with and without FSS the conformal reflector. The figure clearly shows a significant change in the input reflection coefficient value, with an enhancement from -28.35 dB to -38.13 dB at a frequency of 5.9 GHz. Additionally, the antenna's -10 dB bandwidth, which is centered around the 5.9 GHz frequency, measures 230.94 MHz. This narrower bandwidth offers specific advantages for vehicle-to-vehicle (V2V) communication within the dedicated short-range communication (DSRC) system frequency.

Figures 6, 7, and 8 depict the simulation outcomes for the antenna's gain, reflection coefficient, and radiation pattern. A thorough analysis is conducted by comparing the parameters acquired with and without the FSS reflector at  $\phi=0^\circ$  and  $\phi=90^\circ$ . The findings reveal that the presence of the FSS reflector array positioned behind the antenna does not exert a substantial influence on the antenna's transmission coefficient. Moreover, it ensures a commendable impedance adaptation throughout the entire frequency range.

Figures 7(a) and (b) generated at  $\phi=0^\circ$  and  $\phi=90^\circ$  respectively, demonstrate the enhancement of the radiation pattern both with and without the application of FSS. These figures also suggest that the incorporation of FSS could potentially lead to a more focused radiation pattern. This could be particularly beneficial in environments with high levels of interference, thereby improving the reliability and efficiency of V2V communications.

Figure 8 shows the 3D radiation pattern of the patch antenna with the FSS reflector layer, providing a comprehensive view of how the antenna radiates energy in different directions. This visualization clearly demonstrates the influence of the FSS reflector layer on the antenna's radiation characteristics. The pattern reveals enhanced directivity and gain in the desired direction, which is a direct result of the FSS reflector's ability to redirect and focus the electromagnetic waves emitted by the patch antenna.

Figure 9 illustrates a contrast in the enhancements achieved in two scenarios, one with the inclusion of an FSS reflector and the other without. Upon integrating the antenna with the reflector, the gain of the antenna experiences a notable improvement, rising from 3.9 dB to 5.47 dB, which is the peak gain at a frequency of 5.9 GHz. Consequently, the antenna's gain is enhanced and the remaining characteristics remain unaltered.

As depicted in Figure 10, the patch antenna equipped with a FSS demonstrates superior performance compared to conventional designs. Within its operational frequency band, this advanced antenna configuration achieves an efficiency exceeding 67.13%, indicating its high effectiveness in converting input power to radiated power. This remarkable efficiency is a direct result of the FSS integration, which enhances the antenna's ability to focus electromagnetic energy in the desired direction while minimizing losses.

Figure 11 shows that the voltage standing wave ratio (VSWR) for the patch antenna with FSS is 1.025 at a frequency of 5.92 GHz. This value, being less than 2, indicates a good impedance match between the feed line and the antenna. This efficient matching ensures optimal power transfer, thereby enhancing the antenna's performance.

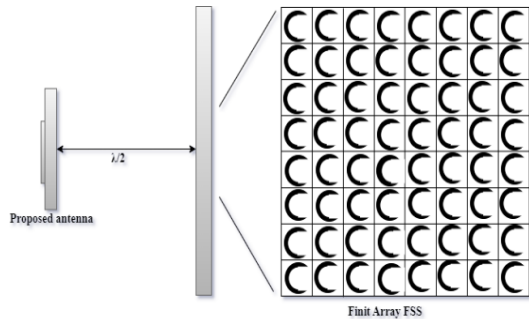


Figure 5. Side profile of antenna with FSS reflector

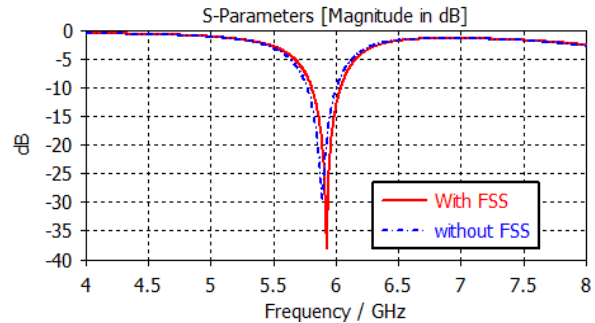


Figure 6. S11 with and without FSS

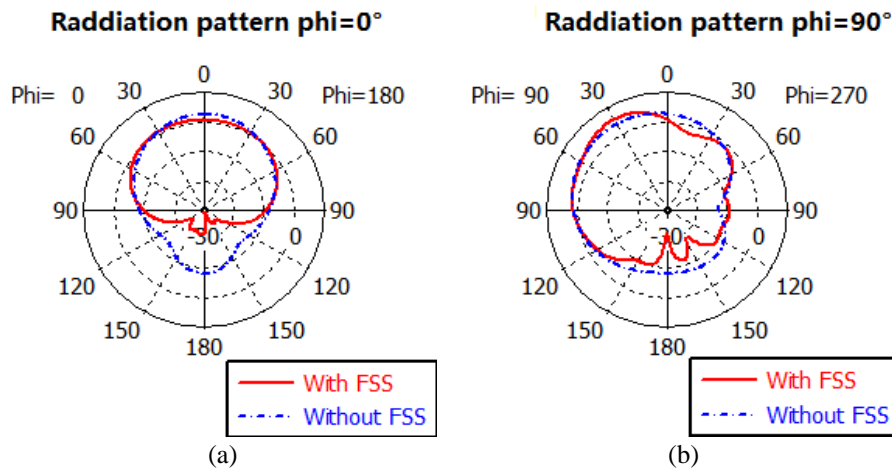


Figure 7. Radiation pattern of antenna (a) Phi=0 and (b) Phi=90°

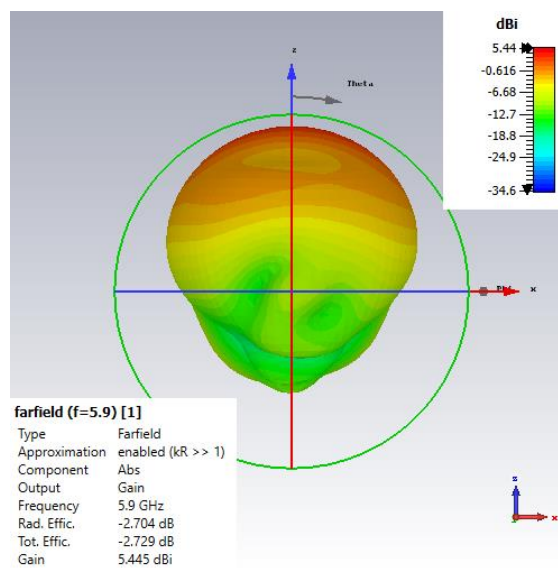


Figure 8. 3D radiation pattern of antenna with FSS

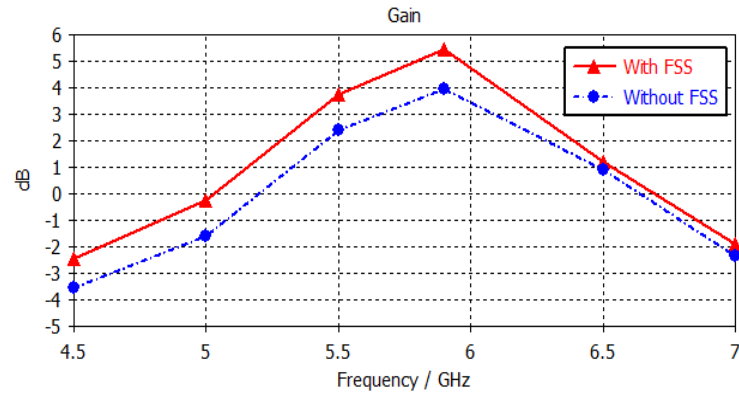


Figure 9. Antenna gain evaluation: impact of FSS

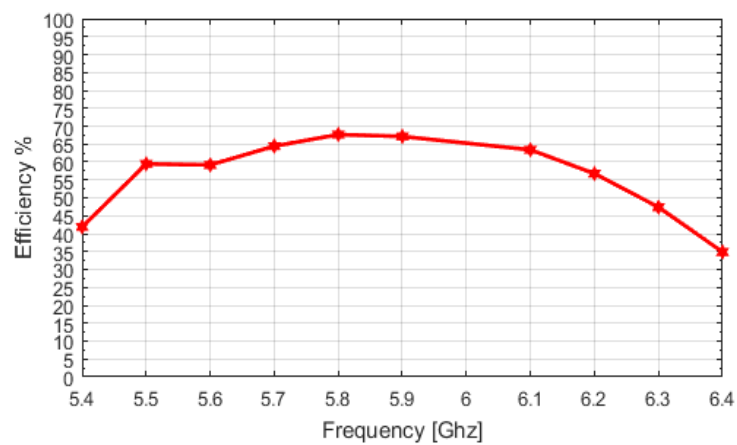


Figure 10. Efficiency of patch antenna with FSS

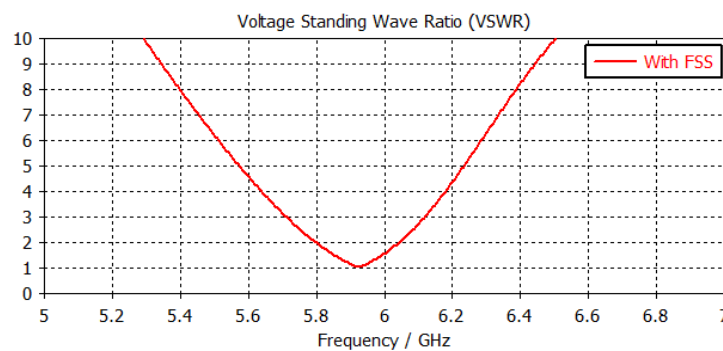


Figure 11. VSWR for patch antenna with FSS

Figure 12 illustrates the far-field characteristics at 5.9 GHz, with subfigures showing the electric field (E-field) and magnetic field (H-field) distributions. Figure 12(a) depicts the E-field pattern in the far-field region, providing insight into the antenna's electric field radiation characteristics at the specified frequency. Complementing this, Figure 12(b) represents the H-field pattern, which offers information about the magnetic field distribution in the far-field. These far-field patterns are crucial for understanding the antenna's radiation behavior, directivity, and overall performance at the 5.9 GHz frequency, which is particularly relevant for vehicle-to-vehicle (V2V) communication applications. By analyzing both the E-field and H-field patterns together, engineers can gain a comprehensive understanding of the antenna's radiation characteristics and make informed decisions about its suitability for specific communication scenarios.

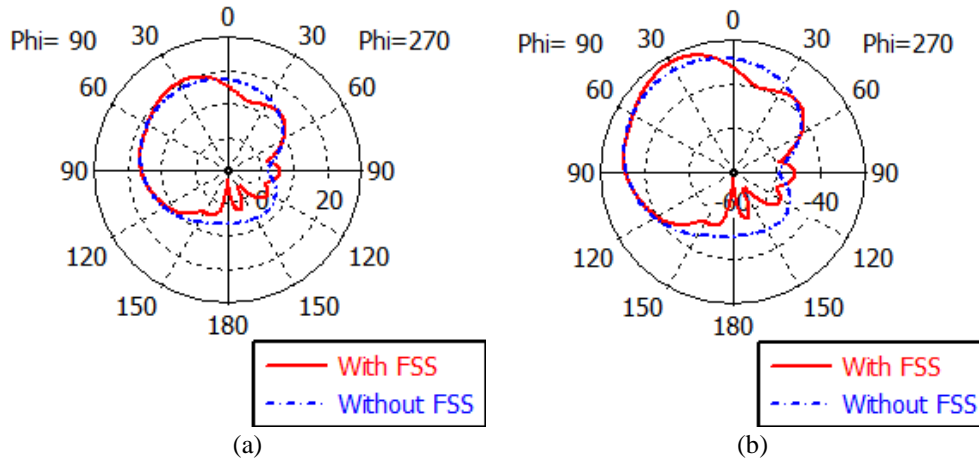


Figure 12. far-Field (a) E-field and (b) H-field at 5.9 GHz

#### 4. VALIDATION RESULTS WITH ADS

In this section, we present the results of the validation of a patch antenna and a FSS using the ADS software. The main objective of this validation is to verify the performance and efficiency of the designed antenna and FSS. ADS, as a cutting-edge electromagnetic simulation tool, allows us to analyze in detail the characteristics of the antenna and the FSS, including the S-parameters. The results obtained from these simulations provide us with valuable information about the behavior of the antenna and the FSS under various conditions, thus helping us to optimize their design for maximum performance.

##### 4.1. Patch antenna with ADS

In Figure 13, the equivalent circuit of a 5.9 GHz microstrip patch antenna, as represented in the ADS platform, is depicted. This figure also includes a screen snapshot of the equivalent circuit of the feed line, which is a real transmission line in the ADS platform. The construction of these equivalent circuits necessitates various parameters such as resistance (R), capacitance (C), and frequency (F). These parameters are integral to the design of the equivalent circuit of both the patch and the feedline of the microstrip patch antenna (as shown in Figure 1). The individual equivalent circuits of the patch and the feedline are subsequently interconnected to form the comprehensive schematic of the patch antennas. This schematic provides a holistic view of the antenna's design and functionality.

Figure 13 illustrates the equivalent circuit and reflection coefficient of the antenna. Figure 13(a) shows the equivalent circuit of the antenna, while Figure 13(b) displays the comparison of the reflection coefficient (S11) for the antenna. In Figure 13(b), the blue line depicts the outcomes obtained from CST electromagnetic simulations, which take into account the intricate nature of the antenna's behavior. On the other hand, the red line represents the circuit equivalent model in ADS, which simplifies the antenna into a circuit with equivalent characteristics. The strong agreement between these two lines confirms the precision of the circuit model, facilitating dependable design and enhancement of the antenna's performance.

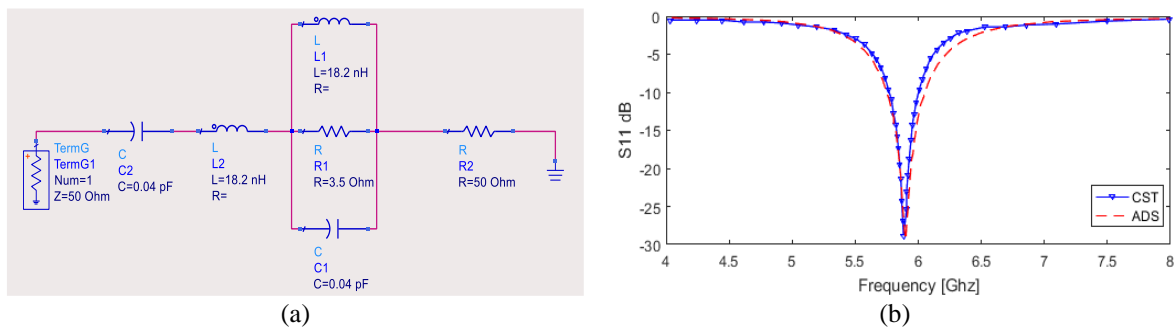


Figure 13. Equivalent circuit and reflection coefficient of the antenna: (a) equivalent circuit of antenna and (b) reflection coefficient of antenna

#### 4.2. FSS with ADS

The equivalent circuit model of FSS can be designed using both ADS and CST software. The equivalent circuit model for FSSs can be deduced and its impedance calculated. The circuit approach is based on an equivalent representation of the FSSs with series or shunt connections of inductances and capacitances. Figure 14 illustrates the equivalent circuit and reflection coefficient of the FSS. Figure 14(a) shows the equivalent circuit of the FSS, while Figure 14(b) displays the comparison of reflection coefficient for the FSS between CST and circuit equivalent with ADS. The results obtained from the ADS simulation, as shown in Figure 14(b), are accurate up to the resonant frequency region of the element. Both lines in Figure 14(b) show similar trends. They descend sharply around 5.9 GHz to reach their minimum values near -55 dB and then ascend. This suggests that the reflection coefficients for FSS between the two methods (CST and ADS) are similar in performance across different frequencies.

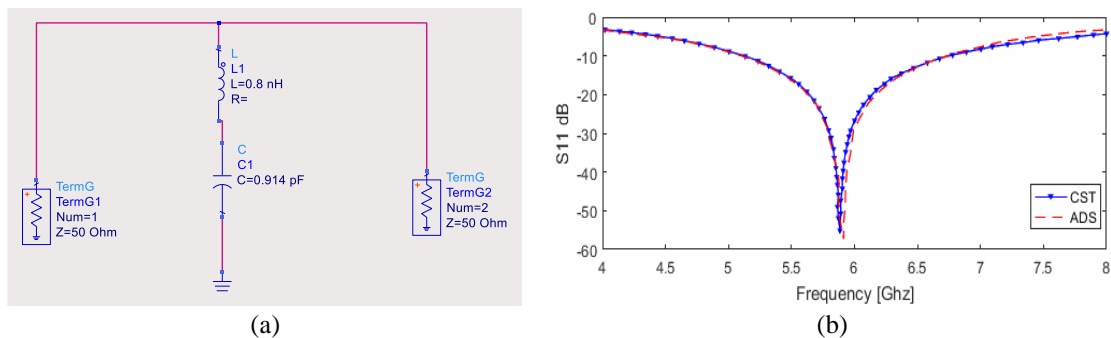


Figure 14. Equivalent circuit and reflection coefficient of FSS: (a) equivalent circuit of FSS and (b) reflection coefficient of FSS

#### 4.3. Antenna patch with FSS implemented in ADS

Figure 15 presents the equivalent circuit and reflection coefficient analysis of a patch antenna with FSS. It utilized two simulation methods, CST and ADS, to analyze a patch antenna with an FSS. Figure 15(a) shows the equivalent circuit of the antenna with FSS, while Figure 15(b) displays the reflection coefficient of the antenna with FSS. The results obtained were consistent across both methods, indicating a high reliability of our simulations. This also demonstrates the accuracy of the models used in both systems to predict the behavior of the patch antenna with FSS. In summary, our work has validated the effectiveness of using CST and ADS for the simulation of patch antennas with FSS.

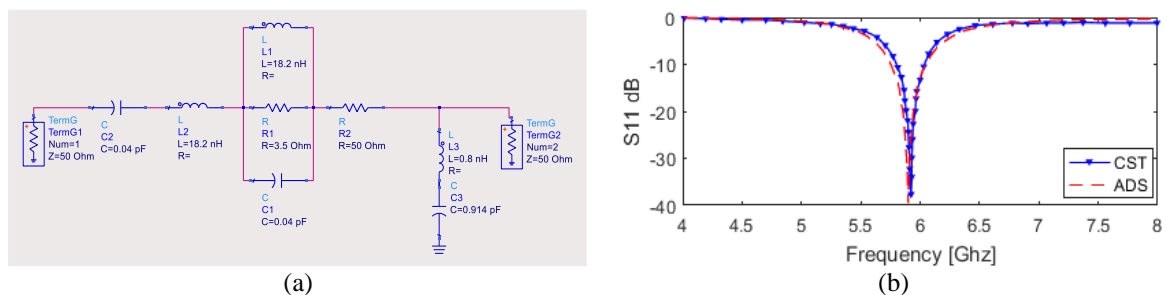


Figure 15. Equivalent circuit and reflection coefficient analysis of patch antenna with FSS: (a) equivalent circuit of antenna with FSS; (b) reflection coefficient of antenna with FSS

### 5. CONCLUSION

In this paper, the study effectively employed a FSS reflector to boost the gain of antennas tailored for vehicle-to-vehicle communications. Integrating the antenna with FSS resulted in a gain enhancement from 3.9 to 5.4 dB at 5.9 GHz, with the bandwidth extending to 230.94 MHz. Notably, the FSS reflector had minimal impact on the antenna's transmission coefficient, ensuring consistent impedance adaptation across the frequency band. These findings underscore the promising potential of FSS in enhancing antenna






performance for V2V applications. Furthermore, when validating these results using an equivalent circuit, we obtained the same outcomes, reinforcing the reliability and accuracy of our study.




## REFERENCES

- [1] M. Aziz, A. El Hassan, M. Hussein, E. Zaneldin, A. H. Al-Marzouqi, and W. Ahmed, "Characteristics of antenna fabricated using additive manufacturing technology and the potential applications," *Heliyon*, vol. 10, no. 6, Mar. 2024, doi: 10.1016/j.heliyon.2024.e27785.
- [2] G. C. Huang, M. F. Iskander, M. Hoque, S. R. Goodall, and T. Bocskor, "Antenna array design and system for directional networking," *IEEE Antennas and Wireless Propagation Letters*, vol. 14, pp. 1141–1144, 2015, doi: 10.1109/LAWP.2015.2391199.
- [3] L. Cheng, K. Huang, Y. Wang, and F. Wu, "Dynamic tunable deflection of radiation based on epsilon-near-zero material," *Photonics*, vol. 10, no. 6, p. 688, Jun. 2023, doi: 10.3390/photonics10060688.
- [4] M. Bayat and J. Khalilpour, "A high gain miniaturised patch antenna with an epsilon near zero superstrate," *Materials Research Express*, vol. 6, no. 4, Jan. 2019, doi: 10.1088/2053-1591/aafe46.
- [5] C. Cheng, Y. Lu, D. Zhang, F. Ruan, and G. Li, "Gain enhancement of terahertz patch antennas by coating epsilon-near-zero metamaterials," *Superlattices and Microstructures*, vol. 139, Mar. 2020, doi: 10.1016/j.spmi.2020.106390.
- [6] G. Singh and A. P. Singh, "On the development of a modified triangular patch antenna array for 4.9 GHz public safety WLAN," *Advanced Electromagnetics*, vol. 8, no. 4, pp. 24–31, Sep. 2019, doi: 10.7716/aem.v8i4.1091.
- [7] S. Akinola, I. Hashimu, and G. Singh, "Gain and bandwidth enhancement techniques of microstrip antenna: a technical review," in *Proceedings of 2019 International Conference on Computational Intelligence and Knowledge Economy, ICCIKE 2019*, Dec. 2019, pp. 175–180, doi: 10.1109/ICCIKE47802.2019.9004278.
- [8] W. El May, I. Sfar, J. M. Ribero, and L. Osman, "A millimeter-wave textile antenna loaded with EBG structures for 5G and IoT applications," *2019 IEEE 19th Mediterranean Microwave Symposium (MMS)*, Hammamet, Tunisia, 2019, pp. 1–4, doi: 10.1109/MMS48040.2019.9157278.
- [9] Y. Alnaiemy and L. Nagy, "Improved antenna gain and efficiency using novel EBG layer," in *SOSE 2020 - IEEE 15th International Conference of System of Systems Engineering, Proceedings*, Jun. 2020, pp. 271–276, doi: 10.1109/SoSE50414.2020.9130494.
- [10] S. Tariq *et al.*, "Frequency selective surfaces-based miniaturized wideband high-gain monopole antenna for UWB systems," *AEU - International Journal of Electronics and Communications*, vol. 170, Oct. 2023, doi: 10.1016/j.aeue.2023.154841.
- [11] T. Tewary, S. Maity, A. Roy, K. Mandal, S. Kundu, and S. Bhunia, "Design and analysis of frequency selective surface embedded broadband high gain miniaturized antenna," *International Journal of Communication Systems*, vol. 37, no. 8, May 2024, doi: 10.1002/dac.5754.
- [12] M. S. Rabbani and H. Ghafouri-Shiraz, "Dual frequency selective surface high gain antenna with deep resonant cavity and E-field reflectors," *Microwave and Optical Technology Letters*, vol. 59, no. 11, pp. 2772–2777, Aug. 2017, doi: 10.1002/mop.30824.
- [13] S. K. R. Vuyyuru, R. Valkonen, D. H. Kwon, and S. A. Tretyakov, "Efficient anomalous reflector design using array antenna scattering synthesis," *IEEE Antennas and Wireless Propagation Letters*, vol. 22, no. 7, pp. 1711–1715, Jul. 2023, doi: 10.1109/LAWP.2023.3260920.
- [14] A. Kapoor, R. Mishra, and P. Kumar, "Frequency selective surfaces as spatial filters: Fundamentals, analysis and applications," *Alexandria Engineering Journal*, vol. 61, no. 6, pp. 4263–4293, Jun. 2022, doi: 10.1016/j.aej.2021.09.046.
- [15] A. Ghaneizadeh, M. Joodaki, J. Borcsok, A. Golmakani, and K. Mafinezhad, "Analysis, design, and implementation of a new extremely ultrathin 2-D-isotropic flexible energy harvester using symmetric patch FSS," *IEEE Transactions on Microwave Theory and Techniques*, vol. 68, no. 6, pp. 2108–2115, Jun. 2020, doi: 10.1109/TMTT.2020.2982386.
- [16] L. Chouikhi, C. Essid, and H. Sakli, "Gain enhancement of monopole antenna using partially reflective surface for 5G application," in *Proceedings - STA 2020: 2020 20th International Conference on Sciences and Techniques of Automatic Control and Computer Engineering*, Dec. 2020, pp. 301–304, doi: 10.1109/STA50679.2020.9329290.
- [17] M. Daghari and H. Sakli, "Radiation performance enhancement of an ultra wide band antenna using metamaterial band-pass filter," *International Journal of Electrical and Computer Engineering (IJECE)*, vol. 10, no. 6, pp. 5861–5870, Dec. 2020, doi: 10.11591/ijece.v10i6.pp5861-5870.
- [18] M. Daghari and H. Sakli, "Antenna radiation performance enhancement using metamaterial filter for vehicle to vehicle communications applications," *Advances in Science, Technology and Engineering Systems*, vol. 5, no. 2, pp. 344–350, 2020, doi: 10.25046/AJ050245.
- [19] R. Yahya, A. Nakamura, and M. Itami, "Ultra-wideband FSS-based antennas," in *UWB Technology and its Applications*, IntechOpen, 2019.
- [20] P. Das, K. Mandal, and A. Lalbakhsh, "Beam-steering of microstrip antenna using single-layer FSS based phase-shifting surface," *International Journal of RF and Microwave Computer-Aided Engineering*, vol. 32, no. 3, Dec. 2022, doi: 10.1002/mmce.23033.
- [21] N. Prasad, P. Pardhasaradhi, B. T. P. Madhav, T. Islam, S. Das, and M. El Ghzaoui, "Radiation performance improvement of a staircase shaped dual band printed antenna with a frequency selective surface (FSS) for wireless communication applications," *Progress in Electromagnetics Research C*, vol. 137, pp. 53–64, 2023, doi: 10.2528/PIERC23072402.
- [22] S. K. Das, B. Champagne, I. Psaromiligkos, and Y. Cai, "A survey on federated learning for reconfigurable intelligent metasurfaces-aided wireless networks," *IEEE Open Journal of the Communications Society*, vol. 5, pp. 1846–1879, 2024, doi: 10.1109/OJCOMS.2024.3378266.
- [23] V. Mishra, M. P. Abegaonkar, L. Kurra, and S. K. Koul, "A configuration of FSS and monopole patch antenna for bidirectional gain enhancement applications," in *2018 IEEE Indian Conference on Antennas and Propagation (InCAP)*, Dec. 2018, pp. 1–4, doi: 10.1109/INCAP.2018.8770781.
- [24] T. Tewary, S. Maity, A. Roy, and S. Bhunia, "Wide band microstrip patch antenna with enhanced gain using FSS structure," *Journal of Microwaves, Optoelectronics and Electromagnetic Applications*, vol. 22, no. 2, pp. 329–345, Jun. 2023, doi: 10.1590/217910742023V22I2273333.
- [25] S. P. Lavadiya *et al.*, "Design and verification of novel low-profile miniaturized pattern and frequency tunable microstrip patch antenna using two PIN diodes," *Brazilian Journal of Physics*, vol. 51, no. 5, pp. 1303–1313, Aug. 2021, doi: 10.1007/s13538-021-00951-2.
- [26] H. Chemkha and A. Belkacem, "Design of new inset fed rectangular microstrip patch antenna with improved fundamental parameters," in *2020 IEEE International Conference on Design & Test of Integrated Micro & Nano-Systems (DTS)*, Jun. 2020, pp. 1–4, doi: 10.1109/DTS48731.2020.9196068.




**BIOGRAPHIES OF AUTHORS**

**Ikram Troudi**    was born in Gafsa Tunisia, in 1995. A Ph.D. student in Genie Engineering at the National School of Engineering of Gabes (ENIG). She received a research master's degree in electronics and telecommunications from the Higher Institute of Computer Science and Multimedia of Gabes (ISIMG), Tunisia, in 2020. She received a Fundamental license in science and technology of information and communication from the Higher Institute of Applied Sciences and Technology of Gafsa (ISSAT Gaf), Tunisia, in 2017. He can be contacted at email: ikram.troudi@isimg.tn.



**Chokri Baccouch**    was born in Gabes Tunisia, in 1988. Assistant professor at Paris 8 University. He received Ph.D. in telecommunications from the National School of Engineering of Tunis (ENIT), Tunisia in 2018. He received the national diploma in engineering telecommunications and networks from the National School of Engineering of Gabes (ENIG), Tunisia, in 2012. Our research works in internet of things, artificial intelligence, communications systems, and harvesting energy. He can be contacted at email: chokribaccouch13@gmail.com.



**Rhaimi Belgacem Chibani**    is an associate professor in Computer Sciences and Information Engineering (CSIE). He joined the National Engineering High School at Gabes named (ENIG) where he is actually employed since Septemer1991. After a doctorate thesis earned at the National Engineering High School at Tunis (ENIT), he received the Ph.D. degree from ENIG, University of Gabes, Tunisia in 1992. He is a member of the Research Laboratory MACS at ENIG as activities supervisor dealing with signal processing and communications research field. Currently, his research areas cover signal processing and mobile communications. He can be contacted at email: abouahmed17@gmail.com.